Arabian Journal of Chemistry (2020) **13**, 5593–5604

King Saud University

Arabian Journal of Chemistry

www.ksu.edu.sa
www.sciencedirect.com

ORIGINAL ARTICLE

Evaluation of structural, spectral characterization and *in vitro* cytotoxic activity studies of some polycyclic aromatic compounds

Majid Rezaeivala [a,*], Koray Sayin [b,c], Serap Şahin-Bölükbaşı [d], Derya Tandoğan [d], Muhammet Kose [e], Aysegül Kose [f]

[a] *Department of Chemical Engeineering, Hamedan University of Technology, Hamedan 65155 Iran*
[b] *Department of Chemistry, Faculty of Science, Sivas Cumhuriyet University, 58140 Sivas, Turkey*
[c] *Advanced Research and Application Center, Sivas Cumhuriyet University, 58140 Sivas, Turkey*
[d] *Department of Biochemistry, Faculty of Pharmacy, Sivas Cumhuriyet University, 58140 Sivas, Turkey*
[e] *Chemistry Department, Kahramanmaras Sutcu Imam University, Kahramanmaras 46100, Turkey*
[f] *Bioengineering and Sciences Division, Kahramanmaras Sutcu Imam University, Kahramanmaras 46100, Turkey*

Received 16 January 2020; accepted 22 March 2020
Available online 4 April 2020

KEYWORDS

Cytotoxic activity;
Polycyclic aromatic compound;
Photoluminescence;
Theoretical Studies

Abstract The present study aims to introduce three known and three new stable polycyclic aromatic compounds synthesized. With MALDI-Mass, ^{1}H and ^{13}C NMR spectroscopy, all new compounds were characterized. In the DMF solution were carried out the electrochemical and photophysical properties of the polyaromatic compounds. The compounds are highly fluorescent showing green-red emission when excited at one single wavelength. For the compound 3, it was shown that the highest Stokes Shift (191 nm) appeared which may be due to the excited state energy transfer. The compounds also indicated the blue-orange region of the electromagnetic spectrum strong emission bands. Additionally, compounds **1, 3, 4,** and **5** were investigated for their *in vitro* cytotoxic activities against PC-3 prostate cancer cells, L-929 non-cancerous cells, and MDA-MB-231 breast cancer for 24 h, 48 h and 72 h. The results obtained from the experiment demonstrated that compounds had different cytotoxic activity against cell lines. Compound **3** was indicated to be inactive against L-929 cells and MDA-MB-231 cancer cells, whereas compounds **1, 4** and **5** indicated a dose and time-dependent cytotoxic activity against PC-3, MDA-MB-231, and L-929 cell lines. It was found that the most sensitive cells to compound **5** were MDA-MB-231 human breast

* Corresponding author.
E-mail address: mrezaeivala@hut.ac.ir (M. Rezaeivala).
Peer review under responsibility of King Saud University.

Production and hosting by Elsevier

https://doi.org/10.1016/j.arabjc.2020.03.021

cancer cells. Additionally, it became clear that compounds **1** and **3** had significant selectivity for human PC-3 prostate cancer cells, and compounds **1, 4** and **5** had considerable selectivity for human MDA-MB-231 breast cancer cells. Also, the quantum chemical examinations of six organic compounds were conducted at the B3LYP/6-31G level in the gas phase and water. According to calculated results, compound 5 was found to be the best candidate for NLO applications.

1. Introduction

Owing to their applications as organic semiconductors for electronic devices, such as organic field-effect transistors (OFETS) (Wang et al., 2011) Light emitting diodes (LEDs) (Tao et al., 2011) and photovoltaic cells (Liu et al., 2013), the synthesis of polycyclic aromatic compounds is extremely interesting. One of the most promising and important approaches is to expand the π electronic system of component molecules, not only to obtain high conductivity (Martoân, 1997), but also to achieve strong effective magnetic coupling (Deuchert and Hünig, 1978). Based on Hunig's classification (Acton et al., 1982), various new π-expanded redox systems have been reported over the last three decades (Martoân, 1997). Nevertheless, the kinetic and thermodynamic stability of the molecule is diminished when a redox active π-electron system is expanded (Wunz et al., 1990, Dorr et al., 2001). Polycyclic aromatic hydrocarbons (PAHs) are regarded as important environmental carcinogens. In addition, different planar ring systems are able to intercalate with DNA, resulting in some drugs possessing chemothera¬peutic activity(Banik and Becker, 2001b). PAHs can be metabolized, are able to interact with cellular components such as protein and nucleic acid, and are soluble in lipid. Carcinogenic properties of PAHs are owing to their metabolic activation (Banik and Becker, 2001b, Bandyopadhyay et al., 2012). For the first time, PAHs-containing anticancer compounds were demonstrated to exist in either the anthracene (Kamal et al., 2004, Bair et al., 1991) or the pyrene ring systems (Hurley, 2002, Henderson and Hurley, 1995, Ingrassia et al., 2009). The use of small molecules disrupting DNA replication and halting rapid cellular division as well as promoting cell apoptosis is one of the major strategies employed in cancer chemotherapy (Kubař et al., 2006). For this purpose, molecules intercalating double-stranded DNA have been demonstrated to be promising as anticancer agents due to the inhibition of topoisomerase enzymes (Jemal et al., 2007, Banik and Becker, 2001a). To have different pharmacokinetics and develop new drugs following the established DNA-intercalation pathway, we need to obtain more information about the drug candidates' physical properties. The presence of a planar aromatic region to contribute to stacking between the DNA bases is the most common structural feature of these DNA intercalators. Although there are various instances of anticancer drug candidates, including naphthalene diimide-based compounds, (Banik et al., 2010) containing extended aromatic regions, their low solubility in aqueous solutions hasve restricted anticancer therapeutic-based applications. Molecules containing an aromatic region in addition to remaining water-soluble are especially effective drug candidates. Considering the fact that studies (Banik et al., 2004, Sayin et al., 2019) have indicated that electrostatic interactions with the negatively charged phosphate backbone of DNA can leverage attractive Columbic intercalation interactions, the two properties are particularly true for cationic DNA intercalators. In the United States, it is well-established that cancer is the leading cause of death in people under the age of 85, and mortality from this disease has increased in recent years (Hartlieb et al., 2015). Thus, it is necessary to develop new strategies and compounds to decrease the mortality and incidence of cancer. It was Ben Mrid et al. who reported *in vitro* cytotoxic activity of the the methanolic extract of Joo needles and berries.The results of which showed potent cytotoxic effects against two breast cancer cell lines (MDA-MB-468 and MCF-7), with no cytotoxicity towards normal cells (PBMCs) (Mrid et al., 2019). In 2019, Ragi and Sivakumar s report came to this conclusion that there was a host-guest inclusion complex of hydroxy propyl β-cyclodextrin (HBCD) and 2-methyl mercapto phenothiazine (2MMPT) and investigated it in liquid state and in solid state. Moreover, *in vitro* cytotoxicity study showed that inclusion of complexation with HBCD did not influence the cytotoxicity of 2MMPT on MCF-7 cell line (Ragi and Sivakumar, 2019). There were obtained two new diterpenoid α-pyrones, named higginsianins A and B, were isolated from the mycelium of the microbial fungus Colletotrichum higginsianum grown in liquid culture as reported by Sangermano et al. (2019). Also, these compounds exhibit cytotoxicity against a broad spectrum of malignant cells which may be regrded as promising anticancer agents (Sangermano et al., 2019). In an other work, the effective anti-inflammatory drug tenoxicam (Ten) and 2,2′-bipyridine (Bipy) Cr(III), Fe(III), Co(II), Ni(II), Cu(II) and Y(III) mixed ligand metal complexes have been informed. The cytotoxicity was screened against cell culture of HCT-116, HepG2 and MCF-7 for all complexes. From the above mentioned results, one can conclude that all the prepared compounds are potent anticancer drug candidates (Mohamed et al., 2019). Recently, we reported the anticancer avtivities of some new morpholine-based ligand and related complexes by using the MTT assay (Rezaeivala et al., 2019). Here, we report the *in vitro* cytotoxic evaluation and the synthesis of certain new polycyclic aromatic compounds (Fig. 1) as a part of previous researches (Lv et al., 2013, Sugiura et al., 2000, Matsui et al., 2007) into synthesized new PAH-bearing anticancer agents. Accordingly, at B3LYP/6-31G level, six organic compounds are optimized in gas phase and water. Then, their NMR spectrum is re-calculated at the same theory level in gas phase. In addition, urea and tetramethylsilane (TMS) are optimized at the same theory level. In the gas phase, non-linear optical properties of linked molecules are investigated. At this stage, a number of quantum chemical descriptors (QCD) are considered.

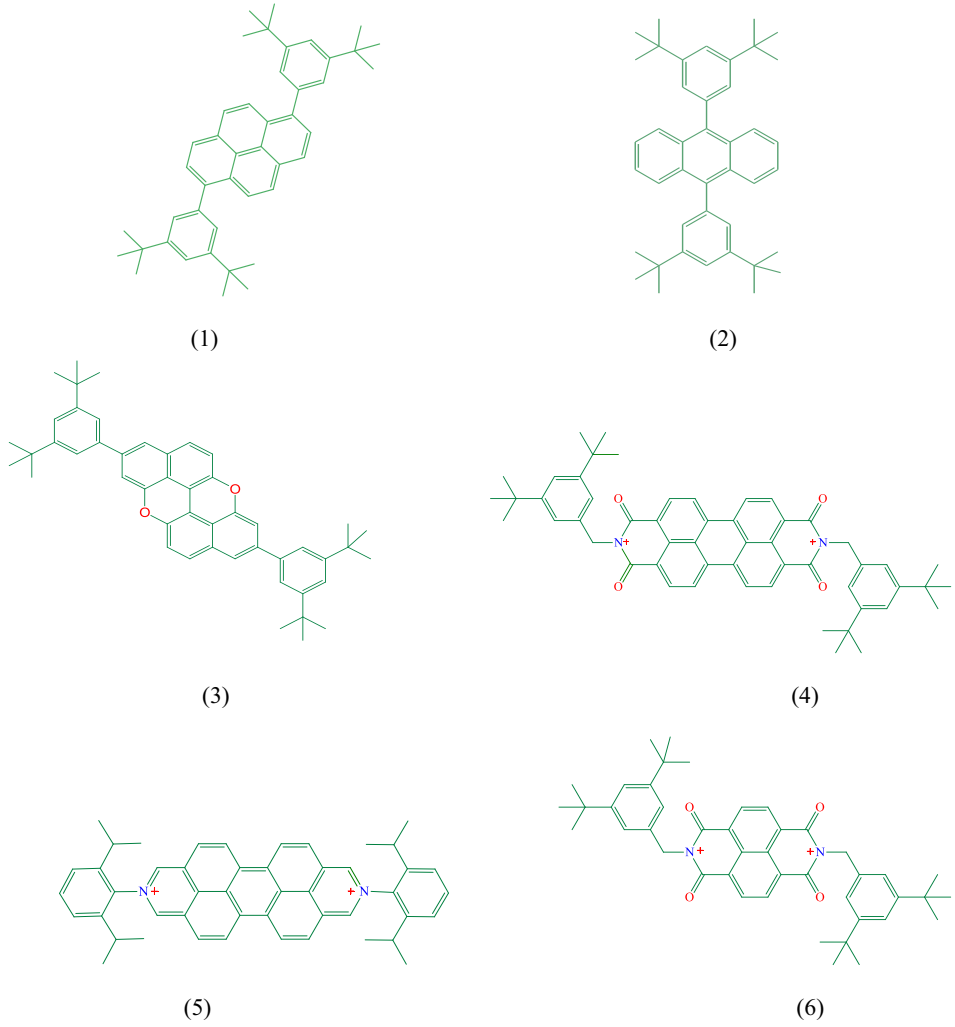

Fig. 1 Molecular structure of compounds.

2. Marterial and methods

General. All reagents and solvents were obtained from commercial sources and used without further purification. Solvents were deoxygenated after Ar were passed through them for 30 min. High-resolution mass spectra (HRMS) were measured on an Agilent 6210 Time of Flight (TOF) LC-MS, using an ESI source, coupled with Agilent 1100 HPLC stack, using direct infusion (0.6 mL/min). Nuclear magnetic resonance (NMR) spectra were recorded on Bruker F500 spectrometers, with the working frequency of 500 MHz. The cyclic voltammetry studies at the glassy carbon electrode were carried out using a BAS 100 W (Bioanalytical System, USA) electrochemical analyser. A glassy carbon working electrode (BAS; Φ: 3 mm diameter), an Ag/AgCl reference electrode (BAS; 3 M KCl) and a platinum wire counter electrode and a standard one-compartment three -electrode cell of 10 mL capacity were used in all experiments. The solutions of the compounds were prepared in DMF (10^{-4} M) for electrochemical studies. The electronic spectra were taken on a Perkin Elmer Lambda 45 spectrophotometer. The fluorescence spectra were obtained on a Perkin Elmer LS55 luminescence spectrometer. Melting points were measured with a Yanako hot stage apparatus without correction.

2.1. Synthesis

2,8-Bis(3,5-di-*tert*-butylphenyl)xantheno[2,1,9,8-*klmna*]xanthene (3) (Fig. SI-13) and 5 (Fig. SI-15) were synthesized as described in the literatures (Lv et al., 2013, Hartlieb et al., 2015).

2.1.1. 1,6-Bis(3,5-di-tert-butylphenyl)pyrene (*1*)

This compound was prepared according to the literature method (Fig. 2) (Sugiura et al., 2000). A mixture of 206.9 mg of 1,6-dibromopyrene and 400 mg of 2-(3,5-di-*tert*-butylphenyl)-4,4,5,5-tetramethyl- [1,3,2] dioxaborolane (2.2 equiv.), 33.2 mg of $Pd(PPh_3)_4$, 1,12 g Cs_2CO_3 and 5 mL of H_2O and dioxane mixture. The reaction mixture was heated with vigorous stirring under nitrogen for 46 h. After being cooled to room temperature, the organic layer was separated and extracted with three 50 mL portions of DCM. The organic phase was dried over $MgSO_4$ and the solvent was removed under the reduced pressure. The dark colored residue was

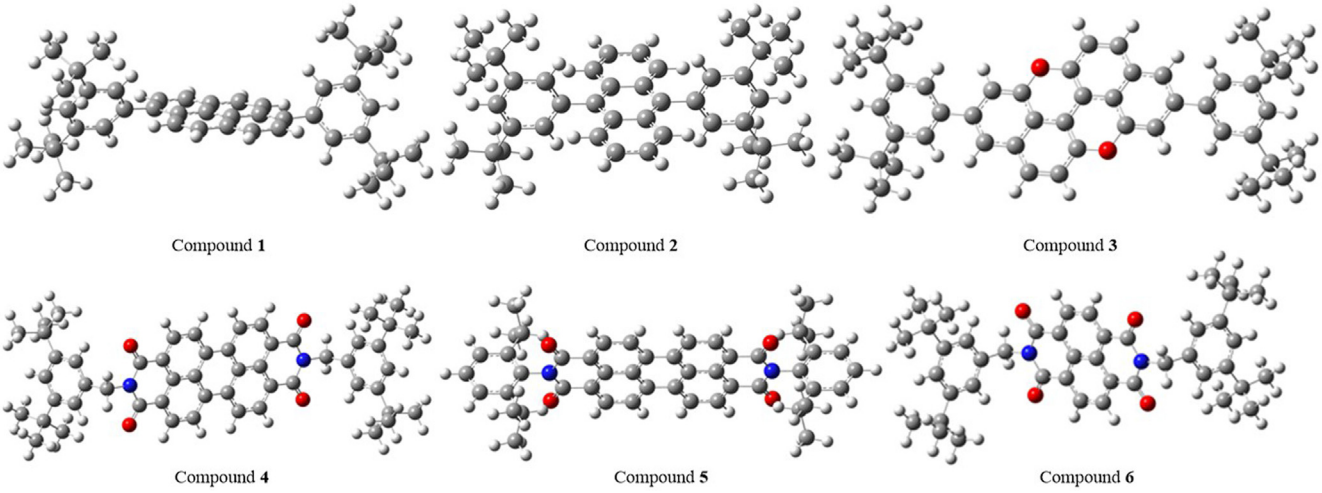

Fig. 2 Optimized structures of organic molecules in gas phase.

chromatographed on SiO_2 eluting with hexane. Crystallization from heptane gave compound (1) (82%). Anal. Calc. for $C_{44}H_{50}$: C, 91.29; H, 8.71; Found: C, 91.43; H, 8.59% (Fig. SI-18).

2.1.2. Synthesis of 9, 10-bis(3,5-di-tert-butylphenyl)anthracene (2)

A mixture of (193.2 mg, 0.575 mmol) of 9,10-dibromoanthracene and of 2-(3,5-di-*tert*-butylphenyl)-4,4,5,5-tetramethyl- [1,3,2] dioxaborolane (400 mg, 1.26 mmol) (2.2 equiv.), (0.0287 mmol, 33.2 mg) of $Pd(PPh_3)_4$, (3.46 mmol, 1,12 g) $CsCO_3$ and 5 mL of H_2O and dioxane mixture. The reaction mixture was heated with vigorous stirring under nitrogen for 48 h. After being cooled to room temperature, the organic layer was separated and extracted with three 50 mL portions of DCM. The organic phase was dried over $MgSO_4$ and the solvent was removed under the reduced pressure. The dark colored residue was chromatographed on SiO_2 eluting with hexane (Fig. 3). Crystallization from heptane gave compound (2) (80%). (Fig. SI-12). UV–Vis in DMF (λ, nm): 343, 361, 382, 482. ^{1}H NMR ($CDCl_3$, 500 MHz): δ = 1.36 (s, 36H), 7.28 (s, 2H), 7.31 (s, 4H), 7.39 (t, J = 7.6 *Hz*, 4H), 7.91 (d, J = 9.2 *Hz*, 4H) (Fig. SI-19). ^{13}C NMR ($CDCl_3$, 500 MHz): δ = 31.98, 34.99, 121.21, 125.35, 126.86, 127.77, 130.25, 131.13, 150.70 (Fig. SI-20).

2.1.3. Synthesis of N, N'-Bis[-di(tert-butyl)benzyl]-3,4:9,10-perylenetetracarboxdiimide (4)

This compound was prepared according to the literature method (Matsui et al., 2007) (Fig. 4). To imidazole suspension (5 mL) of 3,4,9,10-perylenetetracarboxylic dianhhydride (50 mg, 0.125 mmol) were added 3,5-di-*tert*-butylphenyl) methanamine (0.3 mmol) and $Zn(CH_3COO)_2{\cdot}2H_2O$ (17.5 mg, 0.08 mmol). The mixture was heated at 200 °C for 4 h under an argon atmosphere and when the reaction was complete, the reaction mixture was poured into an aqueous solution (10 mL) of saturated sodium hydrogen carbonate, followed by extraction with dichloromethane, and the extract was dried over sodium sulfate (Fig. 4) gave compound (4) (75%). Anal. Calc. for $C_{54}H_{54}N_2O_4$: C, 81.58; H, 6.85; N, 3.52. Found: C, 81.48; H, 6.95; N, 3.63%. MALDI-MS for (4) Calcd for $C_{54}H_{54}N_2O_4$: m/z = 794.408 $[M]^+$; Found: 793.476 $[M-1]^+$ (Fig. SI-14). UV–Vis in DMF (λ, nm): 373, 466, 488, 529. ^{1}H NMR (500 MHz, $CDCl_3$) δ = 1.31 (s, 36H), 5.37 (s, 4H),

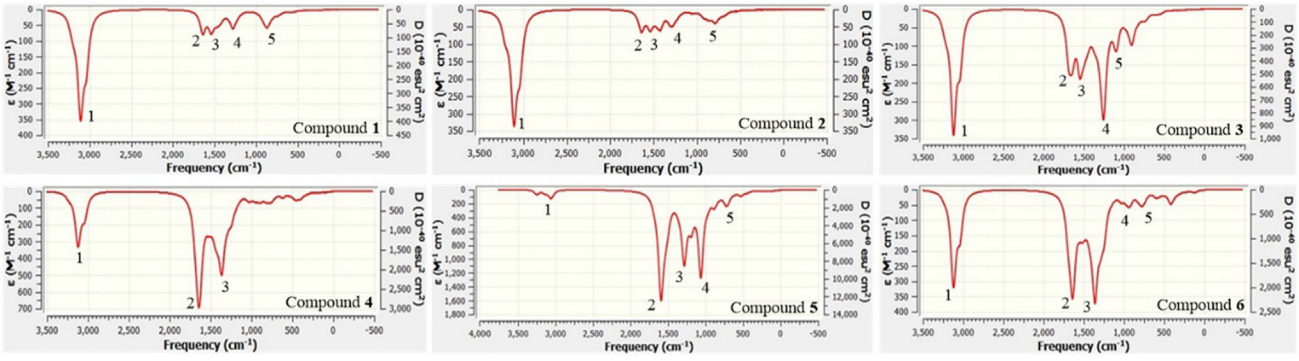

Fig. 3 The IR spectra of related molecules in gas phase.

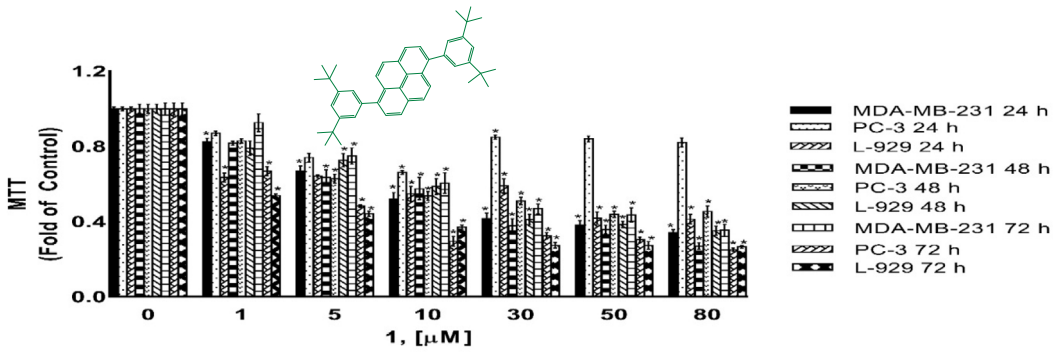

Fig. 4 Cytotoxicity as determined by MTT assay. MDA-MB-231, PC-3 and L-929 cells treated with 1–80 μM of compound **1** for 24 h, 48 h and 72 h. DMSO treated cells were used as vehicle control. Data are representative of the mean ± SE of three separate experiments done in triplicate. (*p < 0.0001 vs control).

7.33 (s, 2H), 7.49 (d, *J = 1.1* Hz, 4H), 8.48 (d, *J = 8.0 Hz*, 4H), 8.62 (d, *J = 8.0 Hz*, 4H) (Fig. SI-21). ^{13}C NMR (500 MHz, $CDCl_3$) δ = 31.49, 34.84, 44.19, 121.80, 123.02, 123.90, 126.13, 128.87, 131.51, 134.59, 136.19, 150.84, 163.36 (Fig. SI-22).

2.1.4. Synthesis of N,N'-Bis[-di(tert-butyl)benzyl]-1,4:5,8-naphthalenetetracarboxdiimide (6)

To imidazole suspension (5 mL) of 1,4,5,8-naphthalenetetracar boxylic dianhydride (50 mg, 0.125 mmol) were added 3,5-di-*tert*-butylphenyl)methanamin (0.3 mmol) and $Zn(CH_3COO)_2 \cdot 2H_2O$ (17.5 mg, 0.08 mmol). The mixture was heated at 200 °C for 4 h under an argon atmosphere and when the reaction was complete, the reaction mixture was poured into an aqueous solution (10 mL) of saturated sodium hydrogen carbonate, followed by the extraction with dichloromethane, and the extract was dried over sodium sulfate (Fig. 5) gave compound (6) (77%). Anal. Calc. for $C_{44}H_{50}N_2O_4$: C, 78.77; H, 7.51; N, 4.18. Found: C, 78.57; H, 7.49; N, 4.38%. MALDI-MS for (6) Calcd for $C_{44}H_{50}N_2O_4$: *m/z* = 670.377 $[M]^+$; Found: 670.635 $[M]^+$ (Fig. SI-16). ^{1}H NMR (500 MHz, $CDCl_3$) δ = 1.28 (s, 36H), 5.35 (s, 4H), 7.33 (s, 2H), 7.45 (s, 4H), 8.74 (b, 4H) (Fig. SI-23). ^{13}C NMR (500 MHz, $CDCl_3$) δ = 31.46, 34.21, 44.42, 121.95, 124.02, 126.78, 131.06, 135.72, 152.34, 162.88 (Fig. SI-24).

3. Computational approaches

Quantum chemical calculations of six organic molecules were performed by Gaussian package programs, GaussView 5.0.8 (Dennington et al., 2009) and Gaussian 09 AM64L-G09RevD.01 (Frisch et al., 2009). Additionally, ChemBioDraw Ultra Version (13.0.0.3015) (Perkinelmer, 2012) program was used as an auxiliary program. In this study, Becke, 3-parameter, Lee-Yang-Parr (B3LYP) was selected as the calculation method and 6-31G was used as the basis set. Urea and tetramethylsilane were selected as reference substances in the investigation of non-linear optical (NLO) properties and nuclear magnetic resonance (NMR) spectrum, respectively. In this study, the energy of the highest occupied molecular orbital (E_{HOMO}), energy of the lowest unoccupied molecular orbital (E_{LUMO}), ionization energy (I), electron affinity (A), energy gap (E_{GAP}), absolute hardness (η), absolute softness (σ), optical softness (σ_O), global softness (S), absolute electronegativity (χ), chemical potential (CP), electrophilicity index (ω), nucleophilicity index (N), additional electronic charges (ΔN_{Max}) and polarizability (α) were used as QCDs. E_{HOMO}, E_{LUMO} and α were directly taken from calculation results. The other descriptors were calculated by using Eqs. (1)–(9) (Serdaroğlu and Mustafa, Sayin and Üngördü, 2018, Shah et al., 2018).

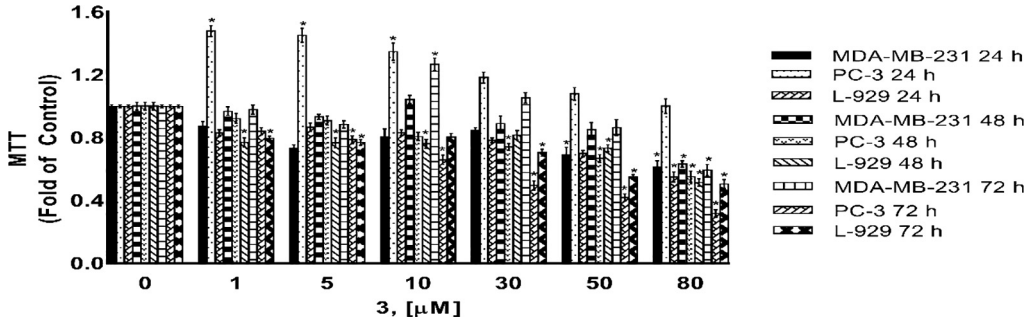

Fig. 5 Cytotoxicity as determined by MTT assay. MDA-MB-231, PC-3 and L-929 cells treated with 1–80 μM of compound **3** for 24 h, 48 h and 72 h. DMSO treated cells were used as vehicle control. Data are representative of the mean ± SE of three separate experiments done in triplicate. (*p < 0.0001 vs control).

$$I = -E_{HOMO} \quad (1)$$

$$A = -E_{LUMO} \quad (2)$$

$$E_{GAP} = E_{LUMO} - E_{HOMO} \quad (3)$$

$$\eta = \frac{I - A}{2} = \frac{E_{LUMO} - E_{HOMO}}{2} \quad (4)$$

$$\sigma = \frac{1}{\eta} \quad (5)$$

$$\sigma_O = \frac{1}{E_{GAP}} \quad (6)$$

$$\chi = \frac{|I + A|}{2} = \frac{|-E_{HOMO} - E_{LUMO}|}{2} \quad (7)$$

$$CP = -\chi \quad (8)$$

$$\Delta N_{Max} = -\frac{CP}{\eta} \quad (9)$$

4. *In vitro* cytotoxic activity

Cell culture; The cells lines MDA-MB-231 (HTB-26, human breast adenocarcinoma), PC-3 (CRL-1435, human prostate adenocarcinoma), fetal bovine serum (FBS, 30-2021), penicillin and streptomycin (30-2300) were purchased from American Type Culture Collection (ATTC, Manassas, VA). Dulbecco's Modified Eagle's Medium (DMEM, D6429) were purchased from Sigma Aldrich. L-929 (normal cells adipose from mouse) were purchased from ECACC (European Collection of Animal Cell Culture, Salisbury, U.K.). All cells were grown in DMEM media containing 10% (v/v) FBS, and 100 Units/ml penicillin and 100 µg/ml streptomycin in a 37 °C humidified incubator with 5% CO_2. Cells were passaged at 70–80% confluence, about twice a week by trypsinization. The passages of all cells lines were no more than 30 during all experiments.

4.1. Cell viability/cytotoxicity assay (MTT assay)

The cytotoxic activities of compounds were determined using MTT (Skehan et al., 1990). Stock solution of the tested compounds were prepared in DMSO and diluted in complete culture medium such that the maximum DMSO content did not exceed 0.5%. Exponentially growing MDA-MB-23, PC-3 and L-929 cells were seeded into 96-well plates at a density of 1×10^5 cells/well and allowed to attach for 24 h before treatment. Then the cells were treated with various concentrations of compounds (1–80 µM), in 5% CO_2, at 37 °C, for 24 h, 48 h and 72 h. The control wells contained cells with media and 0.5% DMSO (final concentration of DMSO) were kept the same in this study. At the end of the exposure period, the cells were subjected to assessment of viability by adopting the MTT assay. 10 µL/well MTT (5 mg/mL, dissolved in phosphate-buffered saline) was added and the cells were incubated for 2 h at 37 °C in 5% CO_2. After removal of the medium and MTT, the purple-blue precipitated crystals were dissolved in 100 µL of DMSO (Sigma, St. Louis, MO). The absorbance was read at 570 nm with Biotek plate reader (Bio-Tek. USA). Evaluation is based on means from at least three independent experiments, each comprising three replicates per concentration level. Their cytotocxic effects were determined in the concentration range 1–80 µM, the dose-response curves were fitted by means of GraphPad Prism 7 (GraphPad Software, San Diego, CA, USA) and the IC_{50} values were calculated.

4.2. Statistical analysis

All experiments were carried out in triplicates with results expressed as means ± SE. Data were analyzed using the one-way analysis of variance and differences were considered significant at $p < 0.0001$. The IC_{50} were determined by statistical software, GraphPad Prism7 (GraphPad Software, San Diego, CA, USA).

5. Results and discussion

5.1. Electrochemical behaviours of the compounds

Cyclic voltammetry studies of the compounds were performed in DMF solution (10^{-4} M) using 0.1 M NBu_4BF_4 as supporting electrolyte. The electrochemical data are given in Table 1. The electrochemical curves of the compounds are shown in (Fig. SI-1–5). At both 100 and 500 mV/s scan rates, compound 1 shows two cathodic peaks at −220 and 230 mV, respectively. In the reverse scan, this compound shows only one anodic peak potential at 90 mV for 500 mV/s and 250 mV for 100 mV/s. The oxidation/reduction peaks at 100 mV/s scan rate is reversible with E_{pa}/E_{pc} = 1.09. The peak potentials at 500 mV/s scan rate are irreversible. As compound 1 and 2 have similar structures, compound 2 shows very similar electrochemical behaviour to compound 1 under the same conditions. At 100 mV/s scan rate, two cathodic peak potentials were observed at – 250 and 190 mV. The first reduction potential is reversible with E_{pa}/E_{pc} = 1.10. The cathodic peak potentials in compound 2 have shifted more negative regions compared to compound 1. At 100 mV/s scan rate, compound 3 have shown three anodic and two cathodic peak potentials in the range of −340/1200 mV. The oxidation peak at E_{pa} = 1200 mV and reduction peak at E_{pc} = 1070 mV are reversible redox couples with E_{pa}/E_{pc} = 1.12. At 500 mV/s scan rate, the compound 3 showed three anodic and two cathodic peak potentials with higher currents. When scan rate was increased to 500 mV/s, the reversible redox potentials became irreversible. When 100 mV/s scan rate was applied, compound 4 has irreversible redox potentials at E_{pc} = −100 mV and E_{pa} = 270 mV. When scan rate was increased to 500 mV/s, the redox potentials became more apparent resulting in a reversible redox potentials E_{pa}/E_{pc} = 1.00. Compound 5 has shown two anodic and two cathodic peak potentials in the range of −430 and 370 mV.

5.2. Absorption and emission properties

Absorption and emission spectra of the compounds (1–5) were investigated in the DMF solution (10^{-5} M) (Figs. SI 5–9 and Table 2). Compound (1) in DMF indicates a broad band in

Table 1 Electrochemical data of the compounds.

Compound	Scan rate (mV/s)	E_{pa} (mV)	E_{pc} (mV)	E_{pa}/E_{pc}	$E_{1/2}$ (mV)	ΔE_p (mV)
1	100	250	−220, 230	1.09	240	20
	500	90	−390, 230	0.39	–	−140
2	100	210	−250, 190	1.10	200	20
	500	80	−330, 210	0.38	–	−130
3	100	−340, 290, 1200	−40, 1070	8.5, 1.12	1035	130
	500	−270, 360, 1350	220, 1030	1.6, 1.31	–	220
4	100	−100	270	−0.37	–	−370
	500	50	−470, 50	1.00	50	0
5	100	−90, 370	−430, 160	0.21, 2.31	–	340, 210
	500	−100, 500	−610, 290	0.16, 1.72	–	510, 210

Table 2 Absorption and excitation/emission maximums for compounds 1–5.

Compound	Absorption (nm)	Excitation (nm)	Emission (nm)	Stokes shift (nm)
(1)	360	355	419	64
(2)	343, 361, 382, 402	370	390, 445	65
(3)	344, 395, 422, 449	281	472, 501	191
(4)	373, 466, 488, 529	524	559, 594	35
(5)	374, 459, 493, 530	527	557, 595	30

the range of 310–390 nm (λ_{max} = 360 nm). The broad absorption band was given to the π → π* electronic transitions of pyrene and phenyl units. Upon excitation at 355 nm with Stokes shift of 64 nm, compound 1 shows a strong emission band at 419 nm (λ_{max}). Owing to the overlapping π → π* electronic transitions of anthracene and phenyl units, compound 2 having an anthracene core unit indicates a number of well-separated absorption bands (λ_{max} = 343, 361, 382 and 482 nm). Compound 2, when excited at 380 nm, exhibits a broad intensive emission band at 445 nm (λ_{max}) with a shoulder band at 390 nm. In the range of 340 and 449 nm, compound 3 has four absorption bands. The bands at 344, 395 and 422 nm (λ_{max}) can be related to π → π* transitions of phenyl and naphthalene moieties. The band at 449 nm (λ_{max}) is assigned to n-π* transitions. Upon excitation at 288 nm, compound 3 has a strong emission band at 450–550 nm (λ_{max} = 472 nm) with a weaker shoulder band at 501 nm. The emission/excitation band of compound 3 indicates a large Stokes shift probably owing to the intramolecular charge transfer within the molecule. In the range of 370–530 nm, compound 4 has four absorption bands. The bands at 373 and 466 nm (λ_{max}) were given to the π → π* transitions of perylene and phenyl units. The next bands at 488 and 529 nm (λ_{max}) may be given to π → π* transitions of di-imide units. Upon excitation at 524 nm with a Stokes shift of 35 nm, compound 4 emits the light in the range of 540–630 nm. Owing to π → π* and n → π* electronic transitions, compound 5 also exhibits four well-separated absorption bands. Compound 5, when excited at 527 nm, exhibits a strong emission band in the range of 520–630 nm (λ_{max} = 557 nm).

The polycyclic aromatic molecules are optimized at B3LYP method with 6-31G basis set in vacuum and water. Their charges are zero expect for compound 5 which has "+2" charge. Electronic structure at ground state in their gas phase is represented in Fig. 6.

According to Fig. 6, there are π electron delocalizations and these molecules are of mainly planar structures except for their aliphatic groups. Bond lengths of C═C in aromatic rings varies between 1.38 and 1.48 Å; C─H lengths is mainly equal to 1.08 Å; C═O lengths in compound **3** is equal to 1.41 Å; C═O bond lengths in compound **4**, **5** and **6** is roughly equal to 1.25 Å; C═N lengths in compound **4**, **5** and **6** is nearly equal to 1.40 Å; C─C lengths in aliphatic groups is nearly 1.54 Å and C─H bond lengths in aliphatic groups is equal to 1.10 Å. According to the published article, the bond lengths of C═C; C═O; C═N; C─C reported to be at the range of 1.370–1.520 Å; 1.197–1.420 Å; 1.497–1.502 Å; 1.523–1.800 Å, respectively [Ishigaki et al., 2018; Lynch and Reeves, 2019; El-Dissouky et al., 2020]. According to the published data, the results in this study are in agreement with the literature.

5.3. Spectral analyses

Characterization of the studied compounds is important to determine some properties which are related with electronic and biological. Through IR spectrum, it is usually possible to determine the functional sites or groups. IR spectra of studied compounds are computed at the same level of theory in the gas phase (Fig. 7). Some peaks in these spectra are labelled the frequencies and vibration modes of which are given in Table 3.

Nuclear magnetic resonance (NMR) is a helpful technique to determine the certain structure. NMR spectra are calculated for each compound. Chemical shift values (in ppm) belonging to carbon and hydrogen atoms are summarized. According to NMR results, the related value of hydrogen atoms linked to aliphatic carbon is between 1.20 and 2.67 ppm; 29–52 ppm for aliphatic carbon atoms; 6.91–10.36 ppm for hydrogen atoms linked aromatic carbon atoms and 107–167 ppm for aromatic carbon atoms.

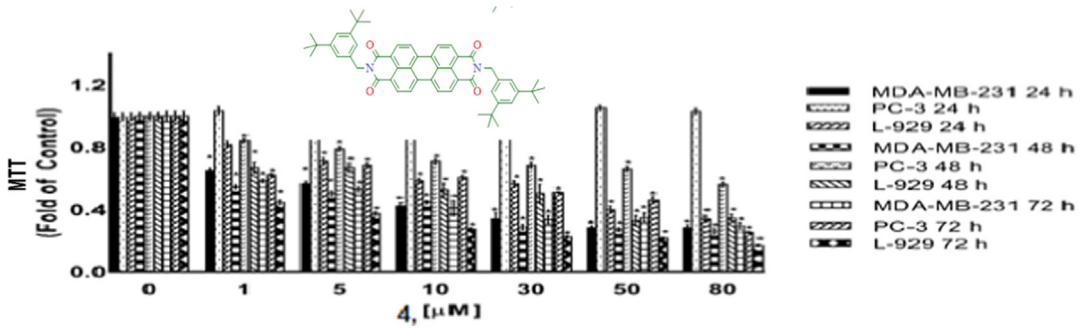

Fig. 6 Cytotoxicity as determined by MTT assay. MDA-MB-231, PC-3 and L-929 cells treated with 1–80 μM of compound **4** for 24 h, 48 h and 72 h. DMSO treated cells were used as vehicle control. Data are representative of the mean ± SE of three separate experiments done in triplicate. (*p < 0.0001 vs control).

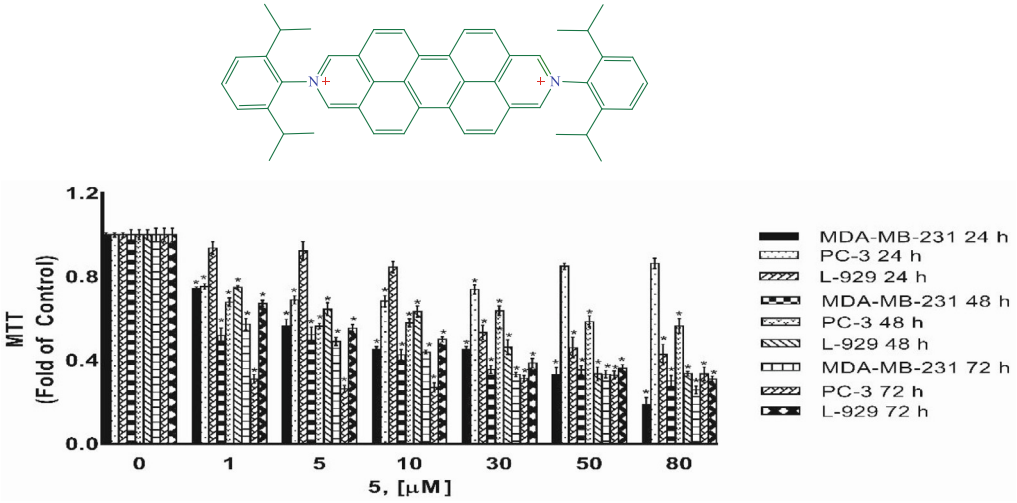

Fig. 7 Cytotoxicity as determined by MTT assay. MDA-MB-231, PC-3 and L-929 cells treated with 1–80 μM of compound **5** for 24 h, 48 h and 72 h. DMSO treated cells were used as vehicle control. Data are representative of the mean ± SE of three separate experiments done in triplicate. (*p < 0.0001 vs control).

Table 3 Frequency (cm^{-1}) and vibrational modes of selected peaks in calculated IR spectra of mentioned compounds.

Compound	1		2		3		4		5	
	Freq.	Mode [a]	Freq.	Mode [a]	Freq.	Mode [a]	Freq.	Mode [a]	Freq.	Mode [a]
Compound **1**	2990	$\upsilon_{CHAliphatic}$	1576	$\upsilon_{C=C}$	1479	$\varsigma_{CH2Aliphatic}$	1229	$\Psi_{CHAromatic}$	837	$\gamma_{CHAromatic}$
Compound **2**	2992	$\upsilon_{CHAliphatic}$	1574	$\upsilon_{C=C}$	1480	$\upsilon_{C=C}$, $\Psi_{CHAromatic}$	1241	$\Psi_{CHAromatic}$	760	$\gamma_{CHAromatic}$
Compound **3**	3003	$\upsilon_{CHAliphatic}$	1587	$\upsilon_{C=C}$	1480	$\varsigma_{CH2Aliphatic}$	1208	υ_{C-C}, $\Psi_{CHAromatic}$	1058	$\upsilon_{C=O}$, $\Psi_{CHAromatic}$
Compound **4**	3001	$\upsilon_{CHAliphatic}$	1581	$\upsilon_{C=O}$, $\upsilon_{C=C}$	1313	$\upsilon_{C=N}$, $\Psi_{CHAromatic}$	–	–	–	–
Compound **5**	2944	$\upsilon_{CHAliphatic}$	1534	$\upsilon_{C=O}$	1235	$\upsilon_{C=N}$, $\upsilon_{C=C}$, $\Psi_{CHAromatic}$	1025	$\upsilon_{C=C}$, $\Psi_{CHAliphatic}$	693	$\gamma_{CHAromatic}$
Compound **6**	3003	$\upsilon_{CHAliphatic}$	1580	$\upsilon_{C=O}$	1312	$\upsilon_{C=N}$, $\Psi_{CHAromatic}$	905	$\gamma_{CHAromatic}$	745	υ_{C-C}

[a] Vibration Modes: υ – stretching; ς – scissoring; ψ – wagging and γ – rocking.

5.4. Nonlinear optical (NLO) properties

NLO are significant features in telecommunications and optical interactions. NLO properties increase with molecular planarity and π electron delocalization. There are molecular planarity and π electrons in studied molecules. Hence, we think that studied molecules have been appropriate in NLO applications. Mentioned QCDs in gas phase are calculated for each compound as given in Table 4.

Table 4 Calculated quantum chemical descriptors at same level of theory in gas phase.

Compound	E_{HOMO}[a]	E_{LUMO}[a]	I[a]	A[a]	E_{GAP}[a]	η[a]
1	−5.327	−1.773	5.327	1.773	3.554	1.777
2	−5.279	−1.834	5.279	1.834	3.445	1.722
3	−4.743	−1.432	4.743	1.432	3.311	1.655
4	−6.121	−3.644	6.121	3.644	2.477	1.238
5	−11.030	−10.726	11.030	10.726	0.304	0.152
6	−6.311	−3.632	6.311	3.632	2.680	1.340
Urea	−6.717	1.471	6.717	−1.471	8.188	4.094
Compound	σ[b]	σ_O[b]	χ[a]	CP[a]	ΔN_{Max}	α[c]
1	0.563	0.281	3.550	−3.550	1.998	574.437
2	0.581	0.290	3.557	−3.557	2.065	518.725
3	0.604	0.302	3.088	−3.088	1.865	581.729
4	0.807	0.404	4.882	−4.882	3.942	684.970
5	6.586	3.293	10.878	−10.878	71.640	1464.636
6	0.746	0.373	4.971	−4.971	3.711	497.470
Urea	0.244	0.122	2.623	−2.623	0.641	24.225

[a] In eV.
[b] In eV^{-1}.
[c] In a.u.

QCDs are helpful in the investigation of activity of chemicals and the relationships between NLO activity of compounds and QCDs have been explained by Sayin et al. in 2018 (Sayin and Üngördü, 2018). The NLO activity ranking as follow for each QCDs:

3 > **2** > **1** > **4** > **6** > Urea > **5** (in HOMO energy)
5 > **4** > **6** > **2** > **1** > **3** > Urea (in LUMO energy)
5 > **4** > **6** > **3** > **2** > **1** > Urea (in E_{GAP})
5 > **4** > **6** > **3** > **2** > **1** > Urea (in absolute chemical hardness and softness)
5 > **4** > **6** > **3** > **2** > **1** > Urea (in optical softness)
Urea > **3** > **1** > **2** > **4** > **6** > **5** (in absolute electronegativity and chemical potential)
5 > **4** > **6** > **3** > **2** > **1** > Urea (in additional electronic charge)
5 > **4** > **3** > **1** > **2** > **6** > Urea (in polarizability)

The mentioned quantum chemical descriptors have been used in many articles to explain the NLO activity of molecules. Especially, the polarizability, energy gap and optical softness are popular parameters maintained for NLO activity [Sayın and Karakaş, 2015; Sayin and Üngördü, 2018; Tüzün and Sayın, 2019]. According to the above ranking, complex **5** seems as the best material via the energy of LUMO, energy gap, absolute chemical softness and hardness, optical softness descriptors. Furthermore, the whole complex results are better than that of urea. According to the above rankings, compound **5** is found to be the best and this compound is a good candidate for NLO applications.

5.5. Cytoxic activity

Compounds 1, 3, 4, and 5 were tested for their cytotoxic activities against MDA-MB-231 breast cancer cell, PC-3 prostate cancer cell and L-929 non-cancerous cells for 24 h, 48 h and 72 h using the MTT assays. MTT assay assess the ability of cells to convert a soluble yellow tetrazolium salt (MTT: 3-(4, 5-dimethylthiazol-2-yl)-2,5-diphenyl tetrazolium bromide) into insoluble purple formazan crystals, which is facilitated by mitochondrial dehydrogenase enzymes. Figs. 8–11 indicating the cytotoxic activities of compounds 1, 3, 4, and 5 on MDA-MB-231, PC-3 and L-929 cells and expressed as IC_{50} (Table 5) which ranged up 1 to 80 μM, suggesting that compounds exhibited cytotoxic activity against cell lines to a different degree. As shown from Table 5, the IC_{50} values varied obviously between different compounds for a certain cell line. A comparison of cytotoxicity between the cell lines identify compounds as selective anticancer agents. According to the IC_{50} values, compound 3 was found to be inactive against MDA-MB-231 cancer cells and L-929 cells but have moderate anti-cancer activity againts PC-3 cancer cells. However, compounds 1, 4 and 5 showed a dose and -time dependent cytotoxic activity against MDA-MB-231 and L-929 cell lines, MDA-MB-231 human breast cancer cells were the most sensitive to the compound 5 (Fig. 7, Table 5). Further, the IC_{50s} for compounds 1, 4 and 5 were higher in non-cancerous L-929 cells compared with the MDA-MB-231 breast cancer cells, suggesting that compounds possessed great selectivity for human MDA-MB-231 breast cancer cells. Although, the cell viability of PC-3 human prostate cancer cells decreased in a dose- and -time dependent base for compouds 1 and 3, compouds 4 and 5 showed anti-cancer activity againts PC-3 cells only for after 72 h treatment. Further, the IC_{50s} for compounds 1 and 3 were higher in non-cancerous L-929 cells compared with the PC-3 prostate cancer cells, suggesting that compounds possessed great selectivity for human PC-3 prostate cancer cells. In contrast to compouds 1 and 3, the IC_{50s} for compounds 4 and 5 were lower in non-cancerous L-929 cells compared with the PC-3 prostate cancer cells. Hartlieb et all. (Hartlieb et al., 2015) were synhesized and investigated the antiproliferative effects of the dichloride salts of the $DAPP^{2+}$ dications 8^{2+} (compounds 5) using a different method. They were used in the concentration of 10 μM of the dichloride and 10 different cancerous cell lines; HT29 (colon), SKMEL-2(melanoma), HepG2 (livercarcinoma),

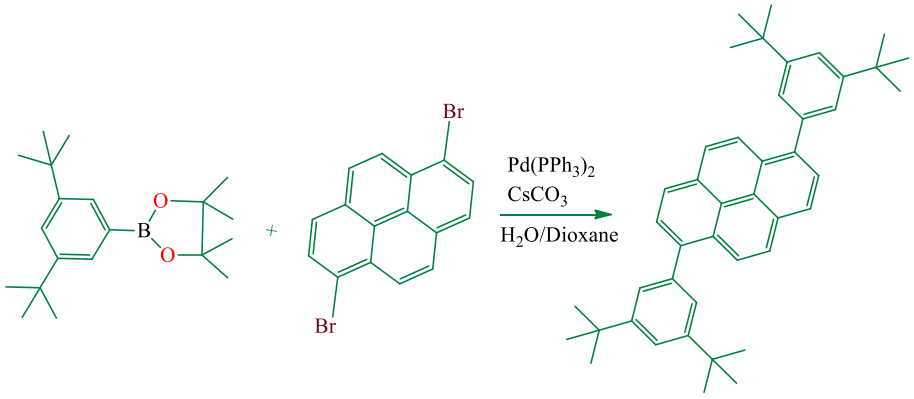

Fig. 8 Synthesis of 1,6-bis(3′,5′-di-*tert*-butylphenyl)pyrene.

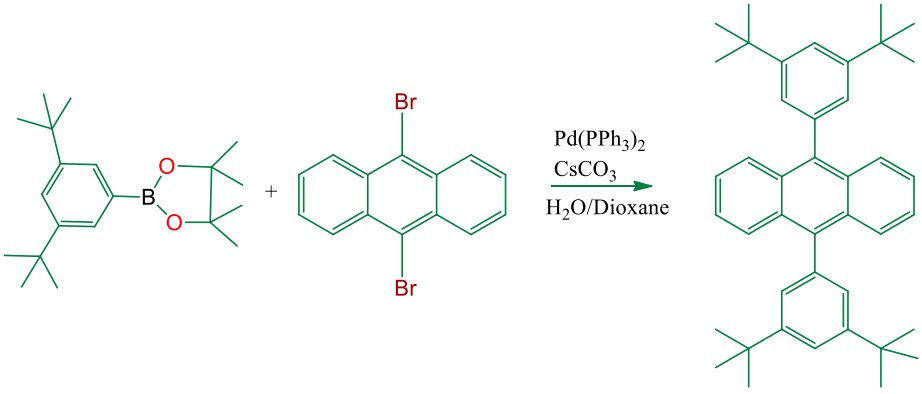

Fig. 9 Synthesis of 9,10-bis(3,5-di-*tert*-butylphenyl)anthracene.

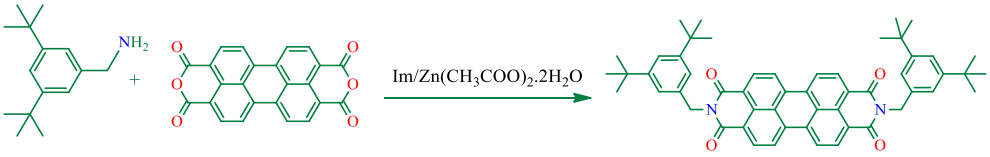

Fig. 10 Synthesis of N,N'-bis[-di(*tert*-butyl)benzyl]-3,4:9,10-perylenetetracarboxdiimide.

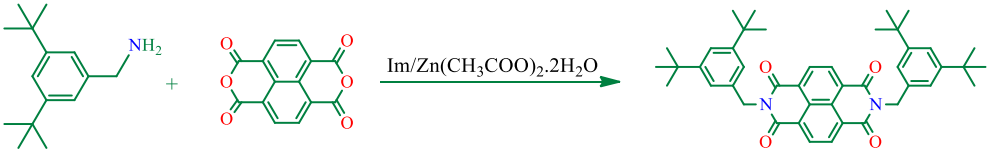

Fig. 11 Synthesis of N,N'-bis[-di(*tert*-butyl)benzyl]-1,4:5,8-naphthalenetetracarboxdiimide.

Jurkat (lymphoma), Hela (cervical), MDA-MB-231 (breast), PC-3 (prostate), FaDu (squamous cell carcinoma), HT1080 (fibrosarcoma), and HL60 (leukemia) for evaluated antiproliferative effects. According to the results of cell proliferation screen, 8 .2Cl exhibited significant potency with less than 50% cell viability, against cell lines (except HepG2 and MDA-MB-231 cells) after a 48 h incubation. But more importantly, 8 . 2Cl exhibited having the lowest cell viability (7.2 ± 2.5%) against SKMEL-2 cell line 10 μM of 8 . 2Cl after a 48 h incubation. 8 . 2Cl showed 66.1 ± 3.5% and 45.6 ± 1.2% cell viability againts MDA-MB-231 and PC-3 cell lines, respectively, when exposed to 10 μM of 8 . 2Cl after a 48 h incubation. In this study we were examined cytotoxic activity of $DAPP^{2+}$ dications 8^{2+} (compounds 5) against MDA-MB-231, PC-3 and L-929 cells for 24 h, 48 h and 72 h using the MTT assays. Our results showed that compoud 5 exhibited (42.5 ± 0.07%) against MDA-MB-231 and (57.8 ± 0.06%) against PC-3 cell viability when exposed to 10 μM

Table 5 Cytotoxic activities of compounds (1, 3, 4 and 5) in selected human cancer and normal cells[a] *in vitro* (IC_{50}, μM[b]) after 24 h, 48 h and 72 h of incubation.

	MDA-MB-231			PC-3			L-929[a]		
Compounds number	24 h	48 h	72 h	24 h	48 h	72 h	24 h	48 h	72 h
1	7.54 ± 0.11	7.44 ± 0.12	5.41 ± 0.13	> 80	6.48 ± 0.17	2.32 ± 0.12	23.6 ± 0.30	12.1 ± 0.13	5.56 ± 0.09
3	> 80	> 80	> 80	> 80	73.6 ± 0.27	34.3 ± 0.14	> 80	> 80	> 80
4	7.88 ± 0.12	7.29 ± 0.12	4.95 ± 0.18	> 80	> 80	52.5 ± 0.18	30.1 ± 0.15	28.8 ± 0.25	< 0.5
5	6.34 ± 0.12	5.52 ± 0.17	2.89 ± 0.15	> 80	> 80	< 0.5	38.7 ± 0.23	28.8 ± 0.13	9.82 ± 0.09

[a] Non-cancer cells.
[b] Cell viability after treatment for 24 h, 48 h and 72 h was determined by MTT staining as described in the Experimental section. Each IC_{50} value represents the mean ± SE of three independent experime.

of compoud 5 after a 48 h incubation. Hartlieb et all. found that IC_{50} values of 8 . 2Cl against SKMEL-2, FaDu and HT-29 cells, 12.3 ± 0.2 μM, 4.81 ± 0.2 μM and 510 ± 260 μM were respectively, while did not observed that IC_{50} values of compoud 5 againts MDA-MB-231 and PC-3 cells. Our results indicated that compound 5 have IC_{50} values on MDA-MB-231 (5.52 ± 0.17 μM) and PC-3 (> 80 μM) cells. These results show that the cytotoxic activities of the compounds may vary depending on which method used.

6. Conclusions

In the present study, we examined the cytotoxic activities of four different compounds. The *in vitro* cytotoxicity studies indicate that compounds can inhibit the cancer cells (MDA-MB-231, PC-3) and non-cancerous cells (L-929) proliferation. Compounds 1, 4 and 5 were observed to display high activities against MDA-MB-231 breast cancer cells, showing much lower cytotoxicity against normal cells adipose from mouse L-929 cells. While, compouns 5 represents highest cytotoxic activity on MDA-MB-231 breast cancer cells, compound 1 represents the highest cytotoxic activity on PC-3 prostate cancer cells. It was observed that the activity of the compound changed depending on the structure of compounds. Furthermore, depending on the composition, the compound was found to be selective for the cancer cell lines. These results direct the focus of our future research program to modify these derivatives which are necessary to improve cytotoxic activity. The compounds are highly fluorescent and showed green-red emission when excited at one single wavelength. Compound 3 showed the highest Stokes Shift (191 nm) and this may be due to the excited state energy transfer. Also, organic compounds are optimized at B3LYP/6-31G level in the gas phase and water. Their optimized structures are obtained from calculations and spectral characterizations are completed. Their NLO properties are investigated in gas phase by using some quantum chemical descriptors. According to the results, NLO properties of related compounds are better than that of urea and compound 5 is found as the best and this compound is a good candidate for NLO applications.

Acknowledgments

We are grateful to the Department of Chemical Engineering Hamedan University of Technology, Ministry of Science, Research and Technology of Iran, for financial support and to the Prof. Sir. J. Fraser Stoddart at Department of Chemistry, Northwestern University for a Visiting Fellowship to M. R in 2016. This research is made possible by TUBITAK ULAKBIM, High Performance and Grid Computing Center (TR-Grid e-Infrastructure). Cytotoxic activity studies were done at Sivas Cumhuriyet University Advanced Technology Application and Research Center (SCUTAM).

Appendix A. Supplementary material

Supplementary data to this article can be found online at https://doi.org/10.1016/j.arabjc.2020.03.021.

References

Acton, N., Hou, D., Schwarz, J., Katz, T.J., 1982. Preparation and oxidation of the bis (tetra-n-butylammonium) salt of 2, 2'-(2, 7-pyrenediyl) bis (propanedinitrile) dianion. J. Organ. Chem. 47, 1011–1018.

Bair, K.W., Andrews, C.W., Tuttle, R.L., Knick, V.C., Cory, M., McKee, D.D., 1991. 2-[(Arylmethyl) amino]-2-methyl-1, 3-propanediol DNA intercalators. An examination of the effects of aromatic ring variation on antitumor activity and DNA binding. J. Med. Chem. 34, 1983–1990.

Bandyopadhyay, D., Granados, J.C., Short, J.D., Banik, B.K., 2012. Polycyclic aromatic compounds as anticancer agents: evaluation of synthesis and *in vitro* cytotoxicity. Oncol. Lett. 3, 45–49.

Banik, B.B., Basu, M.K., Becker, F.F., 2010. Novel disubstituted chrysene as a potent agent against colon cancer. Oncol. Lett. 1, 1033–1036.

Banik, B.K., Becker, F.F., 2001a. Polycyclic aromatic compounds as anticancer agents: structure–activity relationships of chrysene and pyrene derivatives. Bioorg. Med. Chem. 9, 593–605.

Banik, B.K., Becker, F.F., 2001b. Synthesis, electrophilic substitution and structure-activity relationship studies of polycyclic aromatic compounds towards the development of anticancer agents. Curr. Med. Chem. 8, 1513–1533.

Banik, B.K., Becker, F.F., Banik, I., 2004. Synthesis of anticancer β-lactams: Mechanism of action. Bioorg. Med. Chem. 12, 2523–2528.

Ben Mrid, R., Bouchmaa, N., Bouargalne, Y., Ramdan, B., Karrouchi, K., Kabach, I., El Karbane, M., Idir, A., Zyad, A., Nhiri, M., 2019. Phytochemical Characterization, Antioxidant and in vitro Cytotoxic Activity Evaluation of Juniperus oxycedrus Subsp. oxycedrus Needles and Berries. Molecules, 24, 502.

Dennington, R., Keith, T., Millam, J., 2009. GaussView, version 5. Semichem Inc., Shawnee Mission, KS.

Deuchert, K., Hünig, S., 1978. Multistage organic redox systems—a general structural principle. Angew. Chem., Int. Ed. Engl. 17, 875–886.

Dorr, R.T., Liddil, J.D., Sami, S.M., Remers, W., Hersh, E.M., Alberts, D.S., 2001. Preclinical antitumor activity of the azonafide series of anthracene-based DNA intercalators. Anticancer Drugs 12, 213–220.

Frisch, M., Trucks, G., Schlegel, H.B., Scuseria, G., Robb, M., Cheeseman, J., Scalmani, G., Barone, V., Mennucci, B., Petersson, G., 2009. Gaussian 09, revision a. 02, Gaussian. Inc., Wallingford, CT, 200, 28.

Hartlieb, K.J., Witus, L.S., Ferris, D.P., Basuray, A.N., Algaradah, M.M., Sarjeant, A.A., Stern, C.L., Nassar, M.S., Botros, Y.Y., Stoddart, J.F., 2015. Anticancer activity expressed by a library of 2, 9-diazaperopyrenium dications. ACS Nano 9, 1461–1470.

Henderson, D., Hurley, L.H., 1995. Molecular struggle for transcriptional control. Nat. Med. 1, 525–527.

Hurley, L.H., 2002. DNA and its associated processes as targets for cancer therapy. Nat. Rev. Cancer 2, 188.

Ingrassia, L., Lefranc, F., Kiss, R., Mijatovic, T., 2009. Naphthalimides and azonafides as promising anti-cancer agents. Curr. Med. Chem. 16, 1192–1213.

Jemal, A., Siegel, R., Ward, E., Murray, T., Xu, J., Thun, M.J., 2007. Cancer statistics, 2007. CA: A Cancer J. Clinicians 57, 43–66.

Kamal, A., Ramesh, G., Srinivas, O., Ramulu, P., 2004. Synthesis and antitumour activity of pyrene-linked pyrrolo [2, 1-c], benzodiazepine hybrids. Bioorg. Med. Chem. Lett. 14, 471–474.

Kubař, T., Hanus, M., Ryjáček, F., Hobza, P., 2006. Binding of cationic and neutral phenanthridine intercalators to a DNA oligomer is controlled by dispersion energy: quantum chemical calculations and molecular mechanics simulations. Chem.–A Eur. J. 12, 280–290.

Liu, J., Walker, B., Tamayo, A., Zhang, Y., Nguyen, T.Q., 2013. Effects of heteroatom substitutions on the crystal structure, film formation, and optoelectronic properties of diketopyrrolopyrrole-based materials. Adv. Funct. Mater. 23, 47–56.

Lv, N., Xie, M., Gu, W., Ruan, H., Qiu, S., Zhou, C., Cui, Z., 2013. Synthesis, properties, and structures of functionalized peri-xanthenoxanthene. Org. Lett. 15, 2382–2385.

Martoân, N.S.C., 1997. Handbook of Organic Conductive Molecules and Polymers. In: Nalwa, H.S. (Ed.), John Wiley & Sons, Chichester.

Matsui, M., Wang, M., Funabiki, K., Hayakawa, Y., Kitaguchi, T., 2007. Properties of novel perylene-3, 4: 9, 10-tetracarboxidiimide-centred dendrimers and their application as emitters in organic electroluminescence devices. Dyes Pigm. 74, 169–175.

Mohamed, A.A., Sadeek, S.A., El-Hamid, S.M.A., Zordok, W.A., Awad, H.M., 2019. Mixed-ligand complexes of tenoxicam drug with some transition metal ions in presence of 2, 2′-bipyridine: Synthesis, spectroscopic characterization, thermal analysis, density functional theory and in vitro cytotoxic activity. J. Mol. Struct. 1197, 628–644.

Perkinelmer, C.U.V. 2012. CambridgeSoft Waltham. MA, USA.

Ragi, T., Sivakumar, K., 2019. Inclusion Complex of 2-Methyl Mercapto Phenothiazine with Hydroxy Propyl β-Cyclodextrin: Characterization and Cytotoxic Activity Evaluation. Mater. Today:. Proc. 14, 395–408.

Rezaeivala, M., Ahmadi, M., Captain, B., Şahin-Bölükbaşi, S., Dehghani-Firouzabadi, A.A., William Gable, R., 2019. Synthesis, characterization, and cytotoxic activity studies of new N4O complexes derived from 2-({3-[2-morpholinoethylamino]-N3-([pyridine-2-yl] methyl) propylimino} methyl) phenol. Appl. Organometall. Chem., e5325.

Sangermano, F., Masi, M., Vivo, M., Ravindra, P., Cimmino, A., Pollice, A., Evidente, A., Calabrò, V., 2019. Higginsianins A and B, two fungal diterpenoid α-pyrones with cytotoxic activity against human cancer cells. Toxicol. in vitro 61, 104614.

Sayin, K., Kariper, S.E., Taştan, M., Sayin, T.A., Karakaş, D., 2019. Investigations of structural, spectral, electronic and biological properties of N-heterocyclic carbene Ag (I) and Pd (II) complexes. J. Mol. Struct. 1176, 478–487.

Sayin, K., Üngördü, A., 2018. Investigation of anticancer properties of caffeinated complexes via computational chemistry methods. Spectrochim. Acta Part A Mol. Biomol. Spectrosc. 193, 147–155.

Serdaroğlu, G., Mustafa, E.A. Computational study predicting the chemical reactivity behavior of 1-substituted 9-ethyl-βCCM derivatives: DFT-Based Quantum Chemical Descriptors. Turkish Comput. Theor. Chemi. 2, 1–11.

Shah, E.V., Patel, C.M., Roy, D.R., 2018. Structure, electronic, optical and thermodynamic behavior on the polymerization of PMMA: A DFT investigation. Comput. Biol. Chem. 72, 192–198.

Skehan, P., Storeng, R., Scudiero, D., Monks, A., Mcmahon, J., Vistica, D., Warren, J.T., Bokesch, H., Kenney, S., Boyd, M.R., 1990. New colorimetric cytotoxicity assay for anticancer-drug screening. JNCI: J. Natl. Cancer Instit. 82, 1107–1112.

Sugiura, K.-I., Mikami, S., Iwasaki, K., Hino, S., Asato, E., Sakata, Y., 2000. Synthesis, properties, molecular structure and electron transfer salts of 13, 13, 14, 14-tetracyano-1, 6-and-1, 8-pyrenoquinodimethanes (1, 6-TCNP and 1, 8-TCNP). J. Mater. Chem. 10, 315–319.

Tao, Y., Yang, C., Qin, J., 2011. Organic host materials for phosphorescent organic light-emitting diodes. Chem. Soc. Rev. 40, 2943–2970.

Wang, C., Dong, H., Hu, W., Liu, Y., Zhu, D., 2011. Semiconducting π-conjugated systems in field-effect transistors: a material odyssey of organic electronics. Chem. Rev. 112, 2208–2267.

Wunz, T.P., Craven, M.T., Karol, M.D., Hill, G.C., Remers, W.A., 1990. DNA binding by antitumor anthracene derivatives. J. Med. Chem. 33, 1549–1553.